

only LKS stations in NH), are fully consistent with this assumption, particularly for the tropical stations. In the extratropics there are only four daytime-only stations so the MSU test is less meaningful, but the two independent estimates do agree within 0.03°C per decade.

To illustrate the importance of the heating bias, we have computed its impact δ_{sol} on the trends at LKS stations. The LKS f factors, unhomogenized trends, and trends adjusted only for solar heating are given for the middle troposphere and lower stratosphere in Table 2. In the stratosphere, our δ_{sol} is similar to the total adjustments by LKS and others, with trends moving closer to those from MSU (13). At the tropical tropopause (of relevance to stratospheric water vapor), δ_{sol} is somewhat smaller than LKS's. In the troposphere, however, δ_{sol} is much larger than previous adjustments. Indeed, the tropical trend with this adjustment (0.14°C per decade over 1979 to 1997) would be consistent with model simulations driven by observed surface warming, which was not true previously (1). One independent indication that the solar-adjusted trends should be more accurate is their consistency across latitude belts: for the period 1979 to 1997, the spread of values fell by 70% in the lower stratosphere and 25% in the troposphere.

Though this is encouraging, our confidence in these nighttime trends is still limited given that other radiosonde errors have not been addressed. SH trends from 1958 to 1997 seem unrealistically high in the troposphere, especially with the δ_{sol} adjustment, although this belt has by far the worst sampling. Previous homogenization efforts typically produced small changes to mean tropospheric trends, which could mean that other error trends cancel out δ_{sol} in the troposphere. In our judgment, however, such fortuitous cancellation of independent errors is unlikely compared to the possibility that most solar artifacts were previously either missed or their removal negated by other, inaccurate adjustments. To be detected easily, a shift must be large and abrupt, but δ_{sol} was spread out over so many stations (79% of stations during 1979 to 1997 and 90% during 1959 to 1997 experienced ΔT trends significant at 95% level), at such modest levels, and of sufficient frequency at many stations that many may have been undetectable. Most important, jumps in the difference between daytime and nighttime monthly means would be detectable at only a few tropical stations because most lack sufficient nighttime data. In any case, we conclude that carefully extracted diurnal temperature variations can be a valuable troubleshooting diagnostic for climate records, and that the uncertainty in late-20th century radiosonde trends is large enough to accommodate the reported surface warming.

References and Notes

- B. D. Santer *et al.*, *Science* **309**, 1551 (2005); published online 11 August 2005 (10.1126/science.1114867).
- J. K. Angell, *J. Clim.* **16**, 2288 (2003).
- J. R. Lanzante, S. A. Klein, D. J. Seidel, *J. Clim.* **16**, 241 (2003).
- D. E. Parker *et al.*, *Geophys. Res. Lett.* **24**, 1499 (1997).
- P. W. Thorne *et al.*, *J. Geophys. Res.*, in press.
- D. H. Douglass, B. D. Pearson, S. F. Singer, P. C. Knappenberger, P. J. Michaels, *Geophys. Res. Lett.* **31**, L13207 (2004).
- D. J. Gaffen *et al.*, *Science* **287**, 1242 (2000).
- D. E. Parker, D. I. Cox, *Int. J. Climatol.* **15**, 473 (1995).
- M. Free, D. J. Seidel, *J. Geophys. Res.* **110**, D07101 (2005).
- J. K. Luers, R. E. Eskridge, *J. Appl. Meteorol.* **34**, 1241 (1995).
- I. Durrie, T. C. Peterson, R. S. Vose, *J. Clim.* **15**, 1335 (2002).
- L. Haimberger, "Homogenization of radiosonde temperature time series using ERA-40 analysis feedback information," Tech. Rep. European Center for Medium Range Weather Forecasting (2005), ERA-40 Project Report Series 23.
- D. J. Seidel *et al.*, *J. Clim.* **17**, 2225 (2004).
- P. R. Krishnaiah, B. Q. Miao, *Handbook of Statistics*, P. R. Krishnaiah, C. R. Rao, Eds. (Elsevier, New York, 1988), vol. 7.
- M. Free *et al.*, *Bull. Am. Meteorol. Soc.* **83**, 891 (2002).
- W. J. Randel, F. Wu, in preparation.
- D. J. Seidel, M. Free, J. Wang, *J. Geophys. Res.* **110**, D09102 (2005).
- A. Dai, K. E. Trenberth, T. R. Karl, *J. Clim.* **12**, 2451 (1999).
- S. Chapman, R. S. Lindzen, *Atmospheric Tides* (D. Reidel, Norwell, MA, 1970).
- D. R. Easterling *et al.*, *Science* **277**, 364 (1997).
- D. J. Gaffen, R. J. Ross, *J. Clim.* **12**, 811 (1999).
- W. J. Randel *et al.*, *Science* **285**, 1689 (1999).
- K. N. Liou, T. Sasamori, *J. Atmos. Sci.* **32**, 2166 (1975).
- R. E. Eskridge *et al.*, *Bull. Am. Meteorol. Soc.* **76**, 1759 (1995).
- H. Riehl, *Tropical Meteorology* (McGraw Hill, New York, 1954).
- S. C. Sherwood, *Geophys. Res. Lett.* **27**, 3525 (2000).
- J. R. Christy, R. W. Spencer, W. B. Norris, W. D. Braswell, D. E. Parker, *J. Atmos. Oceanic Technol.* **20**, 613 (2003).
- T. Sasamori, J. London, *J. Atmos. Sci.* **23**, 543 (1966).
- Data files and further information on methods, uncertainty, and interpretation of our results are available as supporting material on Science Online.
- S.C.S. thanks J. Risbey and K. Braganza for useful discussions. This work was supported by the National Oceanic and Atmospheric Administration Climate and Global Change Program award NA03OAR4310153, and by NSF ATM-0134893.

Supporting Online Material

www.sciencemag.org/cgi/content/full/1115640/DC1

Methods
SOM Text
Data files
References and Notes

2 June 2005; accepted 27 July 2005

Published online 11 August 2005;

10.1126/science.1115640

Include this information when citing this paper.

The Transcriptional Landscape of the Mammalian Genome

The FANTOM Consortium* and RIKEN Genome Exploration Research Group and Genome Science Group (Genome Network Project Core Group)*

This study describes comprehensive polling of transcription start and termination sites and analysis of previously unidentified full-length complementary DNAs derived from the mouse genome. We identify the 5' and 3' boundaries of 181,047 transcripts with extensive variation in transcripts arising from alternative promoter usage, splicing, and polyadenylation. There are 16,247 new mouse protein-coding transcripts, including 5154 encoding previously unidentified proteins. Genomic mapping of the transcriptome reveals transcriptional forests, with overlapping transcription on both strands, separated by deserts in which few transcripts are observed. The data provide a comprehensive platform for the comparative analysis of mammalian transcriptional regulation in differentiation and development.

The production of RNA from genomic DNA is directed by sequences that determine the start and end of transcripts and splicing into mature RNAs. We refer to the pattern of transcription control signals, and the transcripts they generate, as the transcriptional landscape. To describe the transcriptional landscape of the mammalian genome, we combined full-length cDNA isolation (1) and 5'- and 3'-end sequencing of cloned cDNAs, with new cap-analysis gene expression (CAGE) and gene identification signature (GIS) and gene signature cloning (GSC) ditag technologies for the identification of RNA and mRNA sequences corresponding to transcription initi-

ation and termination sites (2, 3). A detailed description of the data sets generated, mapping strategies, and depth of coverage of the mouse transcriptome is provided in supporting online material (SOM) text 1 (Tables 1 and 2). We have identified paired initiation and termination sites, the boundaries of independent transcripts, for 181,047 independent transcripts in the transcriptome (Table 3). In total, we found 1.32 5' start sites for each 3' end and 1.83 3' ends for each 5' end (table S1). Based on these data, the number of transcripts is at least one order of magnitude larger than the estimated 22,000 "genes" in the mouse genome (4) (SOM text 1), and the

large majority of transcriptional units have alternative promoters and polyadenylation sites. The use of genome tiling arrays (5–7) in humans has also implied that the number of transcripts encoded by the genome is at least 10 times as great as the number of “genes.” To extend the mouse data, two HepG2 CAGE libraries, one constructed with random primers and the other with oligo-dT primers, were combined to produce 1,000,000 CAGE tags. Mapping of these tags to the human genome identified the likely promoters and transcriptional starting site (TSS) of many of the gene models identified by tiling array, also called transfrags (5), and clearly indicates that the same level of transcriptional diversity occurs in humans as in mice (table S2).

The FANTOM Consortium:

P. Carninci,† T. Kasukawa, S. Katayama, J. Gough,† M. C. Frith,† N. Maeda, R. Oyama, T. Ravasi,† B. Lenhard,† C. Wells,† R. Kodzius, K. Shimokawa, V. B. Bajic,† S. E. Brenner, S. Batalov, A. R. R. Forrest, M. Zavolan, M. J. Davis, L. G. Wilming, V. Aidinis, J. E. Allen, A. Ambesi-Impombato, R. Apweiler, R. N. Aturaliya, T. L. Bailey, M. Bansal, L. Baxter, K. W. Beisel, T. Bersano, H. Bono, A. M. Chalk, K. P. Chiu, V. Choudhary, A. Christoffels, D. R. Clutterbuck, M. L. Crowe, E. Dalla, B. P. Dalrymple, B. de Bono, G. Della Gatta, D. di Bernardo, T. Down, P. Engstrom, M. Fagiolini, G. Faulkner, C. F. Fletcher, T. Fukushima, M. Furuno, S. Futaki, M. Gariboldi, P. Georgii-Hemming, T. R. Gingeras, T. Gojobori, R. E. Green, S. Gustincich, M. Harbers, Y. Hayashi, T. K. Hensch, N. Hirokawa, D. Hill, L. Huminiecki, M. Iacono, K. Ikeo, A. Iwama, T. Ishikawa, M. Jakt, A. Kanapin, M. Katoh, Y. Kawasawa, J. Kelso, H. Kitamura, H. Kitano, G. Kollias, S. P. T. Krishnan, A. Kruger, S. K. Kummerfeld, I. V. Kurochkin, L. F. Lareau, D. Lazarevic, L. Lipovich, J. Liu, S. Liuni, S. McWilliam, M. Madan Babu, M. Madera, L. Marchionni, H. Matsuda, S. Matsuzawa, H. Miki, F. Mignone, S. Miyake, K. Morris, S. Mottagui-Tabar, N. Mulder, N. Nakano, H. Nakauchi, P. Ng, R. Nilsson, S. Nishiguchi, S. Nishikawa, F. Nori, O. Ohara, Y. Okazaki, V. Orlando, K. C. Pang, W. J. Pavan, G. Pavesi, G. Pesole, N. Petrovsky, S. Piazza, J. Reed, J. F. Reid, B. Z. Ring, M. Ringwald, B. Rost, Y. Ruan, S. L. Salzberg, A. Sandelin, C. Schneider, C. Schönbach, K. Sekiguchi, C. A. M. Semple, S. Seno, L. Sessa, Y. Sheng, Y. Shibata, H. Shimada, K. Shimada, D. Silva, B. Sinclair, S. Sperling, E. Stupka, K. Sugiura, R. Sultana, Y. Takenaka, K. Taki, K. Tammoja, S. L. Tan, S. Tang, M. S. Taylor, J. Tegner, S. A. Teichmann, H. R. Ueda, E. van Nimwegen, R. Verardo, C. L. Wei, K. Yagi, H. Yamanishi, E. Zabarovsky, S. Zhu, A. Zimmer, W. Hide, C. Bult,† S. M. Grimmond, R. D. Teasdale, E. T. Liu,† V. Brusic, J. Quackenbush,† C. Wahlestedt,† J. S. Mattick,† D. A. Hume†

RIKEN Genome Exploration Research Group and Genome Science Group (Genome Network Project Core Group):

C. Kai, D. Sasaki, Y. Tomaru, S. Fukuda, M. Kanamori-Katayama, M. Suzuki,† J. Aoki, T. Arakawa, J. Iida, K. Imamura, M. Itoh, T. Kato, H. Kawaji, N. Kawagashira, T. Kawashima, M. Kojima, S. Kondo, H. Konno, K. Nakano, N. Ninomiya, T. Nishio, M. Okada, C. Plessy, K. Shibata, T. Shiraki, S. Suzuki, M. Tagami, K. Waki, A. Watahiki, Y. Okamura-Oho, H. Suzuki, J. Kawai.

General Organizer:

Y. Hayashizaki†‡

*Affiliations can be found on Science Online (available at www.sciencemag.org/cgi/content/full/309/5740/1559/DC1).

†These authors are core authorship members.

‡To whom correspondence should be addressed. E-mail: yoshide@gsc.riken.jp

The mapping of ends of transcripts can be used to identify the genomic span of the primary transcript. Figure 1A shows length distributions of the predicted genomic regions spanned by mouse cDNAs showing a bimodal distribution and compares them with one peak for unspliced and another for spliced RNAs. At the upper end of the distribution are candidate mega transcripts (transcripts originating from genomic regions in the order of millions of base pairs). For example, we located six pairs of genome signature cloning (GSC) ditags to RIKEN clone ID 9330159J16 and corresponding RIKEN expressed sequence tags (ESTs). This clone encodes for a previously unidentified large

transcript that is similar to a protein tyrosine phosphatase, receptor type D (accession no. BC086654), the genomic structure of which has not been previously reported (8). The predicted mRNA is 2475 base pairs in length but spans a genomic region of 2.2 megabases (Mb).

We previously coined the term transcriptional units (TUs), which groups mRNAs that share at least one nucleotide and have the same genomic location and orientation (9). However, TU fusions can join unrelated and differently annotated transcripts (SOM text 2). Therefore, we define a transcriptional framework (TK) as grouping transcripts that share common expressed regions as well

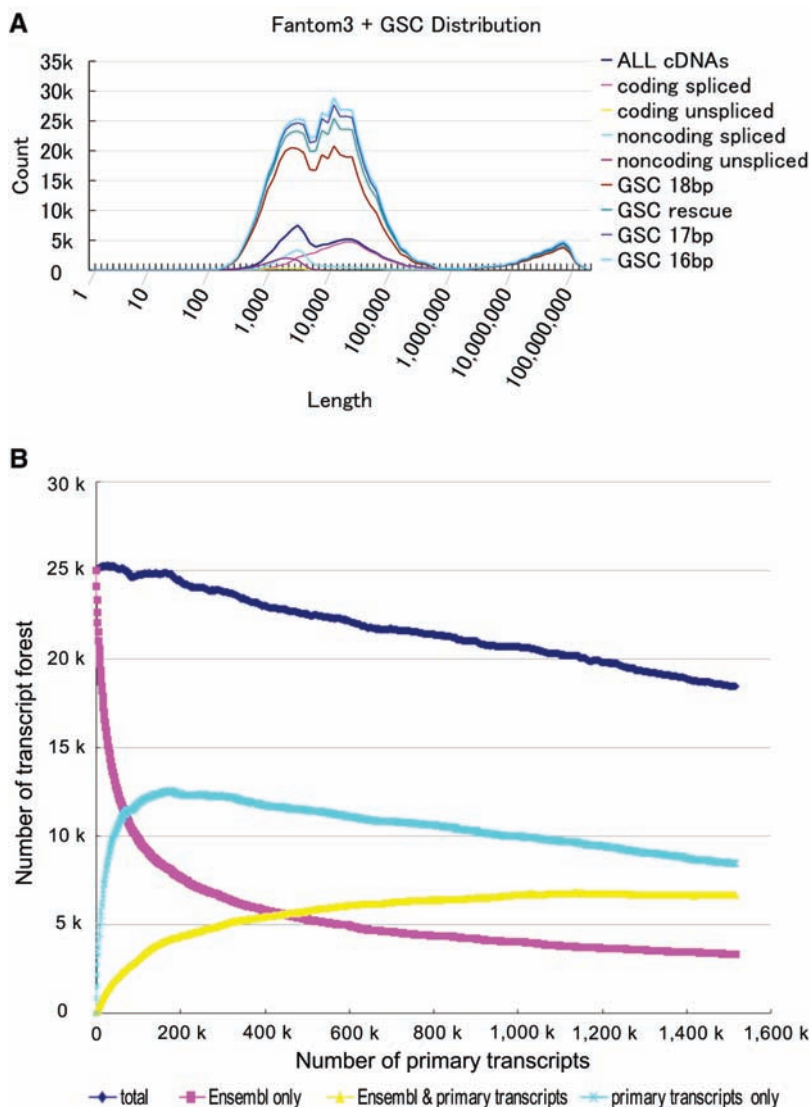


Fig. 1. Genome-transcriptome relation. (A) Genome span covered by full-length cDNA and GIS/GSC ditags shows similar distribution with two main peaks. Ditags mapping follows the same distribution profile at various mapping thresholds, with a minimum around 2 to 2.5 Mb. Mapping events above this genomic span are nonspecific. Count displays the number of events in the size interval. (B) Asymptotic unit collapse. Due to extensive overlap of the genome, transcripts overlap to the extent that they collapse to a few GFs. Simulating addition of ditags shows the collapsing rate of the known annotated genes into 9976 elements only. Primary transcripts only, GFs identified by GSC ditags only; Ensembl only, GFs produced by the 3332 Ensembl-only annotated transcripts; total, the total number of GFs.

as splicing events, TSS, or termination events (SOM text 1).

TKs can be clustered together into transcript forests (TFs), genomic regions that are transcribed on either strand without gaps. TFs encompass 62.5% of the genome (table S1) and are separated by regions

devoid of transcription, or transcription deserts. With the inclusion of GSC tags in addition to full-length cDNA and paired EST sequences, the estimated total number of transcript forests is 18,461, which will collapse further with increasing depth of coverage (Fig. 1B).

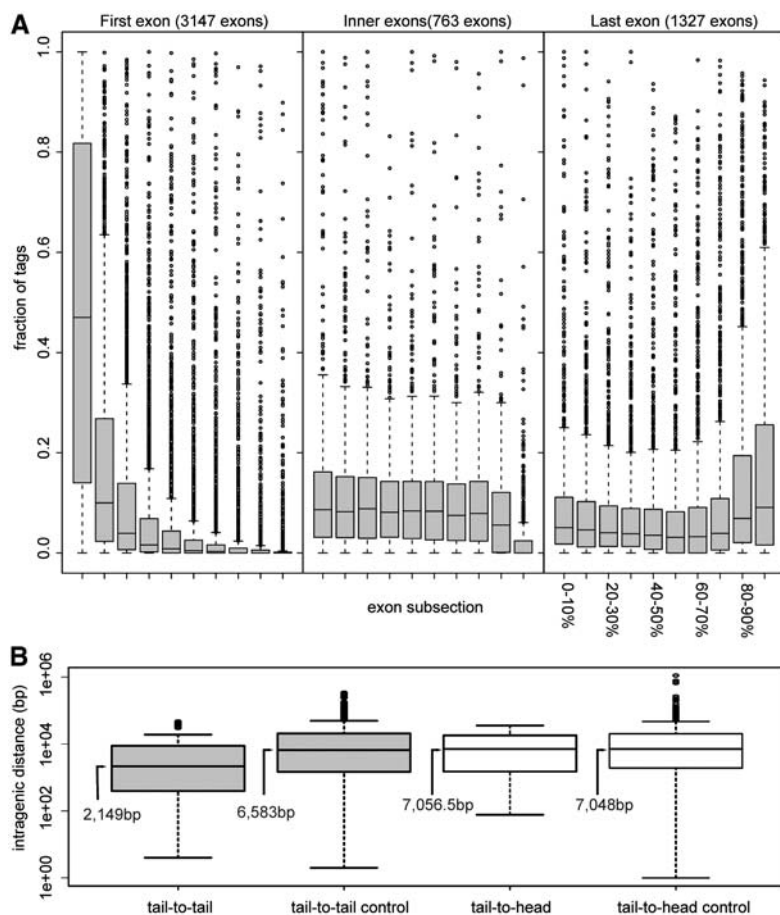


Fig. 2. Transcription originating in 3'UTRs. (A) For each analyzed exon, the fraction of tags mapped to 10 equally large subsections of the exon was calculated. (Left) CAGE tags mapping to the first exon are prevalently located in the first part of the exon. (Middle) CAGE tags mapping to internal exons are uniformly distributed. (Right) Last exons show a distinct overrepresentation of CAGE tags mapping close to the 3' end. (B) Distance to the closest downstream gene for the set of highly expressed TUs that have extreme tag density in the 3' of the terminal exons. Transcript pairs were grouped into tail-to-head (3' exon and downstream TU on same strand) or tail-to-tail (3' exon and downstream TU on opposite strand) configurations. Remaining TUs were used as control groups. For TUs with strong 3' transcriptional activity, the distance to the next TU is significantly smaller than expected when the gene pair is in a tail-to-tail configuration ($P \leq 0.001107$, Wilcoxon test), suggesting regulatory mechanisms based on natural antisense influencing the downstream gene (26).

Table 1. Data set resources.

	Total	Number of libraries	Safely mapped
RIKEN full-length cDNAs	102,801	237	100,313
Public (non-RIKEN) mRNAs	56,009		52,119
CAGE tags (mouse)	11,567,973	145	7,151,511
CAGE tags (human)	5,992,395	24	3,106,472
GIS ditags	385,797	4	118,594
GSC ditags	2,079,652	4	968,201
RIKEN 5'ESTs	722,642	266	607,462
RIKEN 3'ESTs	1,578,610	265	907,007
5'/3'EST pairs of RIKEN cDNA	448,956	264	277,702

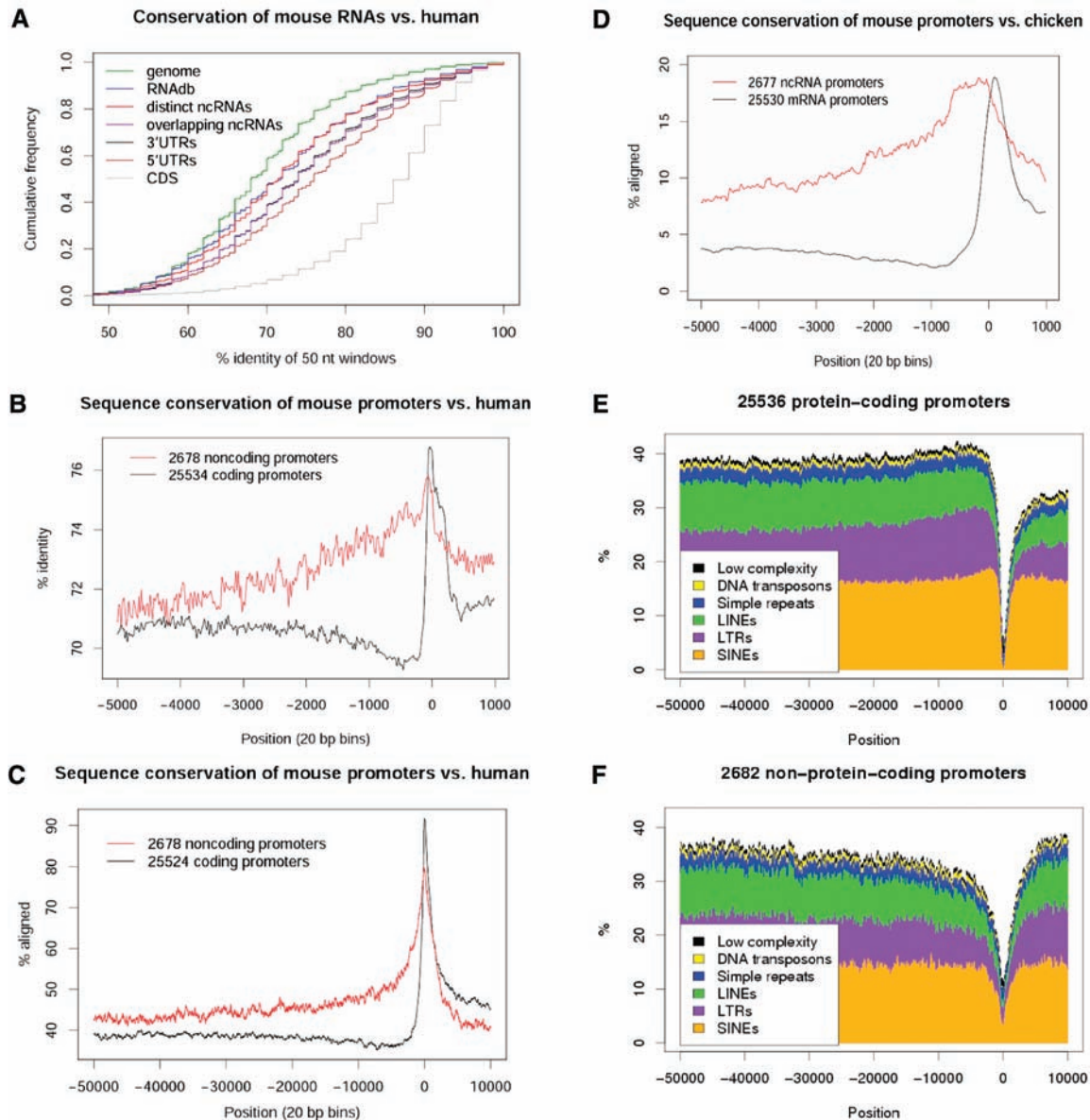
The approach used to isolate full-length cDNAs, based on library subtraction and previously unidentified 5'/3' end selection before full-insert sequencing, was weighted toward identification of representative transcripts. Nevertheless, 78,393 different splicing variants were identified, such that 65% of TUs contain multiple splice variants (Table 2), an increase from our previous estimate (41%) (9). This is still expected to be an underestimate, and new approaches will be necessary for a full evaluation of exon diversity (10).

Transcript diversity also arises through alternative termination. Little is known about sequence motifs that control alternative polyadenylation. We identified 27 motif families with six or more nucleotides that were statistically overrepresented within 120 base pairs of the polyadenylation site of individual transcripts in our data set. These motifs represent candidate modulators of polyadenylation site for eight unconventional alternative polyadenylation signals (1) (table S3). In addition, we found a widespread motif family with sequence TTGTTT, which was associated with both the canonical (AAUAAA and AUUAAA) and unconventional signals (1, 11).

Gene names of 56,722 transcripts that were protein coding were assigned according to annotation rules (9, 12). Their encoded protein sequences were combined with the publicly available proteins supported by cDNA sequences (8). This generated a nonredundant set of 51,135 proteins with experimental evidence [isoform protein set (IPS)], 36,166 of which are complete (complete IPS). By comparison, the mammalian gene collection (<http://mgc.nci.nih.gov>) has cloned, as of July 2005, only ~16,700 transcripts (11,514 nonredundant). In the FANTOM3 data set, 16,274 protein sequences are newly described. Their splice variants were grouped together into 13,313 TKs. For 9002 of these, a previously known sequence maps to the same TK (locus), but 4311 clusters (5154 different proteins) map to new TKs (SOM text 3).

There are a total of 32,129 protein-coding TKs on the genome, of which 19,197 have only a single protein splice form, although 2525 of those do have an alternative noncoding splice variant. The SUPERFAMILY analysis of structural classification of protein database (SCOP) domain architectures (13) was carried out for each sequence. Of the 12,932 TKs that show variation in splicing, 8365 showed variation in SCOP domain prediction. Of the 12,932 variable TKs, 2392 produce proteins with different observed contents of InterPro entries. More than two alternatives were observed in 439 of the 2392 InterPro-variable TKs. Thus, in the majority of variable loci, splicing controls some aspect of domain content or organization. To seek evidence for such an impact in specific sets of regulatory proteins, we compared a representative protein set

Fig. 3. Noncoding RNA promoters are highly conserved. (A) Human-mouse conservation of coding and noncoding RNAs compared with random genome sequence. (B and C) Promoters conserving of noncoding and coding mRNA evaluated (B) by identity and (C) by alignment. (D) Overlap of promoters of ncRNAs. (E and F) Promoters of coding mRNAs contain a larger fraction of low complexity and repeats than noncoding promoters. LINE, long interspersed nuclear elements; LTR, long terminal repeats; SINEs, short interspersed nuclear elements.



(RPS) and a variant protein set (VPS) of phosphatases and kinases that have been comprehensively annotated (14) by looking at domain composition counts (table S4). These phosphoregulators could be functionally modulated through alteration in their intracellular location. Among the 21 receptor tyrosine phosphatase loci, we identified 23 variant transcripts from 14 loci with predicted changes to the subcellular localization and function of the encoded peptides. Of these, we identified two noncatalytic classes: secreted (10) and tethered (3). Furthermore, we identified two catalytic classes that lack the extracellular domains: catalytic only (5) and tethered catalytic (5). Similarly, among the 77 receptor kinase loci, we identified 41 variant transcripts from 33 loci which encode secreted (16), tethered (10), catalytic only (7), or other tethered catalytic (8) peptides. We then analyzed the membrane organization splicing

variants class within the full set of TUs (table S5), which revealed 1287 TUs that exhibit alternative initiation, splicing, and termination, likely to yield variant isoforms of membrane proteins that differ in their cellular location.

Of the 102,281 FANTOM3 cDNAs, 34,030 lack any protein-coding sequence (CDS) and are annotated as non-protein coding RNA (ncRNA) (6, 15) (table S1). Many putative ncRNAs were singletons in the full-length cDNA set. Among the FANTOM3 cDNA set there was additional support from ESTs, CAGE tags, or other cDNA clones overlapping both the starting and termination sites for 41,025 cDNAs, of which only 3652 were ncRNAs. This supported ncRNA set includes many known ncRNAs (SOM text 4), and many are dynamically expressed (SOM text 5). Following these same criteria, 3012 from 8961 cDNAs previously annotated as truncated

CDS were supported as genuine transcripts and are believed to be ncRNA variants of protein-coding cDNAs.

Many ncRNAs appear to start from initiation sites in 3' untranslated regions (3'UTRs) of protein-coding loci (16). The normalized distribution of CAGE tags along annotated exons of known transcripts with more than 300 mapped tags each is shown in Fig. 2A. As expected, the highest tag density on average occurs at the 5' end, but there is also a substantial increase of tags in the last one-fifth of the 3'UTR. Strong evidence of 3' end initiation was correlated with a short intergenic distance when in tail-to-tail orientation with a neighboring gene (Fig. 2B), suggesting a possible role in an intergenic regulatory interaction.

The function of ncRNAs is a matter of debate (17). Some ncRNAs are highly conserved even in distant species: 1117 out of 2886

Table 2. Transcript grouping and classification. The extent of splice variation was calculated by excluding T-cell receptor and immunoglobulin genes from the transcripts. The remaining 144,351 transcripts were grouped in 43,539 TUs, of which 18,627 (42.8%) consist of single-exon transcripts, 8110 (18.6%) contain a single multiexon transcript, and the remaining 16,802 TUs (38.6%) contain at least two spliced transcripts. Among these TUs, 5862 (34.9%) show no evidence of splice variation, whereas 10,940 (65.1%) contain multiple splice forms.

	Total	Average per TU cluster	Average per TK cluster
Total number of transcripts	158,807	7.59	7.30
RIKEN full-length	102,801		
Public (non-RIKEN) mRNAs	56,006		
GFs	25,027	1.20	1.15
Framework clusters	31,992	1.53	1.47
TUs	44,147	2.11	2.03
With proteins	20,929	1.00	0.96
Without proteins	23,218	1.11	1.07
TK	45,142	2.16	2.07
With proteins	21,757	1.04	1.00
Without proteins	23,385	1.12	1.07
Splicing patterns	78,393	3.75	3.60

Table 3. Determination of transcripts start/end accuracy. Two pieces of evidence (cDNA, tags, ditags, EST, and 5'-3' EST pairs) are required when TSS/terminations lie inside larger transcripts, and one piece of evidence is required when they extend or identify new transcripts. Reliable indicates that both ends are associated with reliable tag clusters.

	Total	Reliable
Total 5'/3'-end pair sequence	1,507,122	1,336,397
5'/3'-end pair cluster	313,821	181,047

overlap chicken sequences, of which 780 do not overlap known CDS and 438 do not overlap known mRNAs on either strand, whereas 68 out of 2886 have BLAST-like alignment tool (BLAT) alignments to the Fugu genome, of which 40 do not overlap known CDS on either strand. These ncRNAs are at least as conserved as a reference set of known ncRNAs (Fig. 3A), contrary to a previous study (17). However, ncRNAs are slightly less conserved on average than 5' or 3'UTRs. In contrast, the promoter regions of ncRNAs are generally more conserved than the promoters of the protein-coding mRNA, not only between human and mouse but also down in the evolutionary scale to chicken (Fig. 3, B to F), and they contain binding sites for known transcription factors (18). We conclude that the large majority of ncRNAs that we analyzed display positional conservation across species. In considering function, one might conclude that the act of transcription from the particular location is either important or a consequence of genomic structure or sequence (for example, enhancers such as that of the globin locus can act as promoters), the transcript may function through some kind of sequence-specific interaction with the DNA sequence from which it is derived, or many noncoding

RNAs have other targets but are evolving rapidly (19, 20).

New databases have been created for cDNA annotation, expression, and promoter analysis (<http://fantom3.gsc.riken.jp/db/> and SOM text 6). The databases integrate common gene and tissue ontologies like eVOC mouse developmental ontologies (21), cross mapped to Edinburgh Mouse Atlas Project (EMAP) ontology terms (22). These eVOC terms allow analysis standardization of RNA samples used for cDNA and CAGE libraries in both mouse and human and were included into the DNA Database of Japan (DDBJ) data submission (23).

Analysis of the output of FANTOM2 suggested that there were many more transcripts still to be discovered (24). Here, we have confirmed that the majority of the mammalian genome is transcribed, commonly from both strands. Such transcriptional complexity implies caveats in interpretation of microarray experiments (25) and genome manipulation in mice, because these will commonly interrupt or interrogate more than one TK. Although the current overview gives us an indication of the complexity of the mammalian transcriptional landscape and a new set of tools to begin to understand transcriptional control (for example a very large set of promoters that can be ascribed to distinct classes) (16), we also gain insight into the scale of the task that remains. The ditag data indicate the existence of very long transcripts whose isolation and sequencing will require new cloning and sequencing strategies. Although we have isolated and sequenced many putative ncRNAs, the FANTOM3 collection only contains 40% of those already known. Finally, the focus has been on polyadenylated mRNAs that are processed and exported to the cytoplasm. Recently, Gingeras and colleagues (5) have

shown that the set of nonpolyadenylated nuclear RNAs may be very large, and that many such transcripts arise from so-called intergenic regions (7). The future can only reveal additional complexity in the mammalian transcriptome.

References and Notes

1. P. Carninci *et al.*, *Genome Res.* **13**, 1273 (2003).
2. T. Shiraki *et al.*, *Proc. Natl. Acad. Sci. U.S.A.* **100**, 15776 (2003).
3. P. Ng *et al.*, *Nat. Methods* **2**, 105 (2005).
4. R. H. Waterston *et al.*, *Nature* **420**, 520 (2002).
5. D. Kampa *et al.*, *Genome Res.* **14**, 331 (2004).
6. P. Bertone *et al.*, *Science* **306**, 2242 (2004).
7. J. Cheng *et al.*, *Science* **308**, 1149 (2005).
8. R. L. Strausberg *et al.*, *Proc. Natl. Acad. Sci. U.S.A.* **99**, 16899 (2002).
9. Y. Okazaki *et al.*, *Nature* **420**, 563 (2002).
10. A. Watahiki *et al.*, *Nat. Methods* **1**, 233 (2004).
11. V. Bajic, in preparation.
12. N. Maeda, R. Oyama, in preparation.
13. J. Gough, in preparation.
14. A. R. Forrest *et al.*, *Genome Res.* **13**, 1443 (2003).
15. Materials and methods are available as supporting material on Science Online.
16. P. Carninci *et al.*, in preparation.
17. J. Wang *et al.*, *Nature* **431**, 1 p following 757; discussion following 757 (2004).
18. S. Cawley *et al.*, *Cell* **116**, 499 (2004).
19. T. Ravasi, D. A. Hume, in *Encyclopedia of Genetics, Genomics, Proteomics, and Bioinformatics*, L. B. Jorde, P. F. R. Little, M. J. Dunn, S. Subramaniam, Eds. (John Wiley & Sons, Chichester, UK, in press), part 2.3.
20. J. S. Mattick, I. V. Makunin, *Hum. Mol. Genet.*, in press.
21. J. Kelso *et al.*, *Genome Res.* **13**, 1222 (2003).
22. R. A. Baldock *et al.*, *Neuroinformatics* **1**, 309 (2003).
23. All sequences (CAGE, and cDNA) are available through DDBJ to other public databases. The cDNA clones are available.
24. Y. Okazaki, D. A. Hume, *Genome Res.* **13**, 1267 (2003).
25. E. Marshall, *Science* **306**, 630 (2004).
26. RIKEN Genome Exploration Research Group and Genome Science Group (Genome Network Project Core Group) and the FANTOM Consortium, *Science* **309**, 1564 (2005).
27. We thank H. Atsui, A. Hasegawa, Y. Hasegawa, K. Hayashida, H. Hirai, F. Hori, T. Iwashita, S. Kanagawa, C. Kawazu, M. Aoki, K. Murakami, M. Murata, H. Nishida, M. Nishikawa, K. Nomura, M. Ohno, Y. Onodera, N. Sakazume, H. Sato, Y. Shigemoto, N. Suzuki, Y. Takeda, Y. Tsujimura, K. Yoshida for discussion, encouragement, and technical assistance. We thank A. Wada, T. Ogawa, M. Muramatsu, and all the members of RIKEN Yokohama Research Promotion Division for support and encouragement. We also thank the Laboratory of Genome Exploration Research Group for secretarial and technical assistance, Yokohama City University for providing human samples, and computational resources of the RIKEN Super Combined Cluster (RSCC). This work was mainly supported by Research Grant for the Genome Network Project from MEXT, the RIKEN Genome Exploration Research Project from MEXT (Y.H.), Advanced and Innovative Research Program in Life Science (Y.H.), National Project on Protein Structural and Functional Analysis from MEXT (Y.H.), Presidential Research Grant for Intersystem Collaboration of RIKEN (P.C. and Y.H.) and a grant from the Six Framework Program from the European Commission (P.C.).

Supporting Online Material

www.sciencemag.org/cgi/content/full/309/5740/1559/DC1
 Materials and Methods
 SOM Text
 Figs. S1 to S4
 Tables S1 to S10
 References
 DDBJ Accession Codes

9 March 2005; accepted 4 August 2005
 10.1126/science.1112014